Journal of Nanobiotechnology

RESEARCH Open Access

Alternating magnetic field-responsive engineered probiotics for anxiety therapy via gut-brain axis modulation

Xuejun Wang[1], Yuhan Zhang[1], Yuling Chang[1], Yuhao Zhu[1], Guo Xiang[2], Kehua Chen[2], Chuanxing Feng[1], Zhaofang Hang[1], Xingang Li[1,2,3*] and Di Zhang[1,2,3*]

Abstract

The discovery of the gut-brain axis demonstrated bidirectional regulation between the gut and the brain. The gastrointestinal branches of the vagal nerve have been proven to directly modulate multiple functions of the central nervous system (CNS), providing great opportunities to develop novel tools to remotely regulate CNS function from the gut. Engineered bacteria, acting as oral live biotherapeutics, offer a durable and controllable way of modulating neuronal function non-invasively and with low side effects. Here, we constructed an engineered bacterium by genetically modifying *Escherichia coli* Nissle 1917 (EcN) with Fe_3O_4 nanoparticles to release gamma-aminobutyric acid (GABA) under the control of the alternating magnetic fields (AMF). Bioavailability, assessed by survival rate in artificial gastric fluid, was further enhanced by encapsulating EcN with a poly-norepinephrine (NE) layer, which protected the probiotics from environmental stress and improved their viability during oral delivery. The oral administration of the EcN-GadABC@Fe-NE/AMF in restraint mice exhibited significant anxiolytic efficacy, which was attenuated by the chemogenetic counteraction of vagal sensory inhibition. Immunohistochemistry staining against c-fos showed reduced neuronal activation in both the nucleus of the solitary tract (NTS) and locus coeruleus (LC) area in the restraint mice treated by the EcN-GadABC@Fe-NE/AMF. Furthermore, acting as a probiotic, the EcN-GadABC@Fe-NE modulated gut microbiota homeostasis, additionally contributing to the alleviation of anxiety-like behaviors. This approach opens up a novel revenue for developing remote and non-invasive methods to modulate CNS function from the gut, and enhancing bacteriotherapy for mental disorders.

*Correspondence:
Xingang Li
lixg@sdu.edu.cn
Di Zhang
dizhang@sdu.edu.cn
[1]Jinan Microecological Biomedicine Shandong Laboratory, Jinan 250017, PR China
[2]Department of Neurosurgery, Qilu Hospital, Cheeloo College of Medicine, Institute of Brain and Brain-Inspired Science, Shandong University, 107 Wenhuaxi Rd, Jinan 250012, PR China
[3]Shandong Key Laboratory of Brain Health and Function Remodeling, Jinan 250017, PR China

Graphical abstract

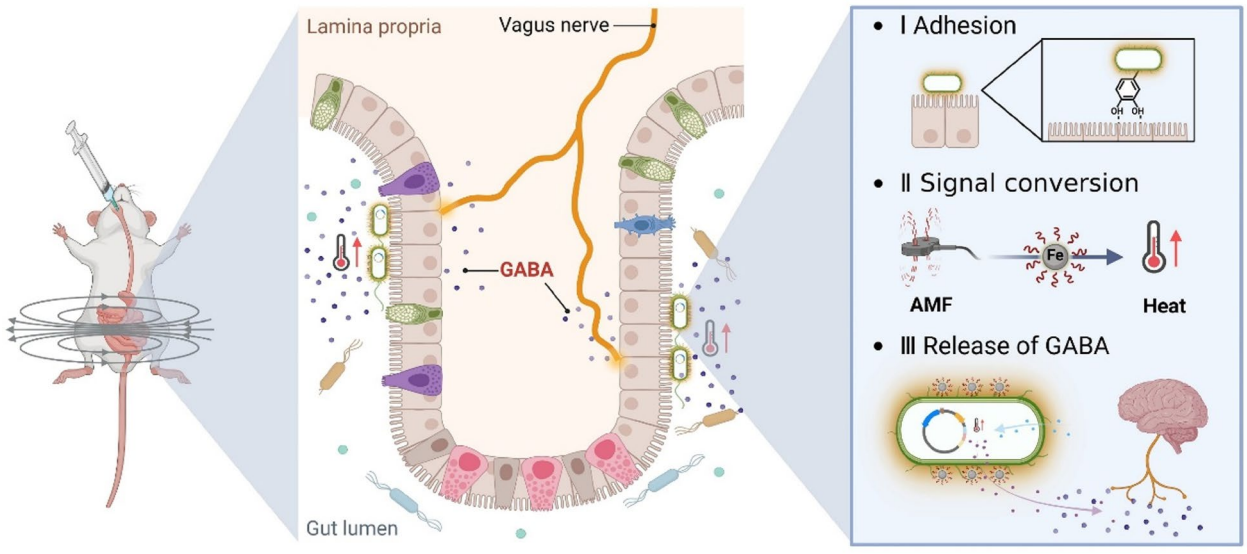

Keywords Gut-brain axis, Engineered bacteria, Anxiety therapy, Gastrointestinal vagal afferents, Nanomaterials

Introduction

Anxiety disorders, characterized by excessive, persistent, and unrealistic worry affect over 300 million individuals per year [1]. Severe anxiety disorders can lead to suicide attempts [2], which have serious consequences for individuals and society. Therefore, there is an urgent need for treatment to address anxiety disorders. Patients with anxiety disorders often display somatic and visceral sensations, leading to dysfunctional body-brain interoception [3–5]. As a key body-brain axis in interoception, the afferents of the vagus nerve, which compose 80% of the vagus nerve [6], transmit signals from visceral organs into the brain, positioning it as a potential target for therapeutic intervention for anxiety disorders.

The intestinal microbiota acting through the neuro–endocrine–immune pathways form the gut-brain axis, which is closely associated with the development of anxiety disorders [7]. The gastrointestinal innervating afferents of the vagal nerve are the major and direct nerve connections between the gut and the brain and have long been recognized as the core of the gut-brain axis ([6, 8] – [9]). Despite its conventional role in conducting meal-borne signals and feedback inhibition on food intake [10, 11], the gastrointestinal vagal afferents (GVA) are demonstrated to be involved in modulating several higher cerebral functions including mood and anxiety through the nucleus of the solitary tract (NTS) [12–15]. Pathogenic bacteria in rodents can induce anxiety-like behaviors, which are mediated via GVA [16, 17]. In addition, vagus nerve stimulation elicits corticosterone release [18] and subdiaphragmatic vagal deafferentation significantly reduces innate anxiety-like behavior [19]. Further evidence using designer receptors exclusively activated by designer drugs (DREADD) demonstrated that inhibition of the GVA exhibited pronounced anxiolytic effects [13], positioning GVA inactivation as a potential approach for alleviating anxiety-like behaviors. Gamma-aminobutyric acid (GABA), a common inhibitory neurotransmitter, can be produced by gut microbes. Moreover, the nerve terminals of the GVA located at the submucosal layer of the gastrointestinal tract express a significant amount of GABA receptors [20], which introduces a new way to regulate anxiety-like behaviors from the gut by bacteria-mediated GVA inactivation.

The advantages of efficient targeted delivery in vivo, continuous and stable production of bioactive factors, as well as flexibility in design, have enabled the development of engineered bacteria for targeted drug delivery against various diseases, including cancer, intestinal inflammation, and metabolic diseases [21–23]. Subsequent modification of the engineered bacteria with nanomaterials facilitated the development of multifunctional strains, achieving precise spatiotemporal control and improved bioavailability. For example, bacteria were engineered for the synthesis of capsular polysaccharides and programmable encapsulation to evade immune attack and increase bacterial bioavailability in the circulation and translocation to the tumor sites [24]. In addition, Guo et al. designed an engineered *Lactobacillus casei* (Se-fLac) containing selenium dots to enhance the bacterium's

gastric acid resistance and intestinal adhesion when orally administered [25]. Therefore, the versatility of nanomaterial-modified engineered bacteria holds great potential for neuromodulation of gastrointestinal innervating vagal afferents.

Herein, we designed a nanomaterial-assisted engineered bacteria system with controlled release of GABA in response to the alternating magnetic field (AMF) stimulation, for modulation of gastrointestinal innervating vagal afferents to achieve anxiolytic effects and evaluated its efficacy in a mouse model of anxiety (Fig. 1). The system was constructed with three modules: the modified *Escherichia coli* Nissle 1917 (EcN) with plasmid pBV220-pRpL-GadABC to release GABA through temperature control; coated Fe_3O_4 nanoparticles onto the outer membrane of the EcN to convert the magnetic signal into the thermal signal to induce the controllable production and release of GABA upon AMF stimulation; and the poly-norepinephrine (poly-NE) layer to protect the EcN against the environmental assaults and to enhance its mucosal adhesion. The nanomaterial-assisted engineered bacteria system (EcN-GadABC@Fe-NE) enables the controlled release of GABA under AMF stimulation and prolonged retention time of engineered bacteria in the intestine. The biochemical characterization and functional evaluation of the system were conducted, and the mechanisms of action were explored. Using chemogenetic manipulation and immunohistochemistry staining, we found that the EcN-GadABC@Fe-NE could exert anxiolytic effects through synergically inactivation of NTS and LC area. At the same time, 16 S rRNA results showed the restoration of gut microbiota dysbiosis by oral administration of EcN-GadABC@Fe-NE in mice. The nanomaterial-assisted engineered bacteria system proposed an effective and steerable way for gut-brain axis modulation and a potential therapeutic strategy for mood disorders.

Materials and methods

Materials

The main chemicals and biological material used in this study are listed below: trypsin (Sigma-Aldrich), pepsin (Thermo Fisher Scientific), bile salts (Sigma-Aldrich), Norepinephrine (Sigma-Aldrich), kanamycin (Sigma-Aldrich), Luria Broth (LB, Fisher Bioreagents), agar (Fisher Bioreagents), $FeCl_3 \cdot 6H_2O$ (Sigma-Aldrich), $FeCl_2 \cdot 4H_2O$ (Sigma-Aldrich), Cell Count Kit-8 (CCK-8, Apexbio), 1-Ethyl-3(3-dimethylaminopropyl) carbodiimide (EDC, Energy Chemical), N-hydroxysuccinimide (NHS, Energy Chemical), CGP35348 (Sigma-Aldrich). Simulated gastric fluid (SGF) and simulated intestinal fluid (SIF) were prepared as described in the United States Pharmacopoeia. To prepare SGF, 2.0 g of NaCl and 3.2 g of pepsin were dissolved in 1 L of DI water, and the pH was adjusted to 1.5 with HCl. The SGF was filtered by a 0.22-μm membrane before usage. SIF was prepared by dissolving 6.8 g of KH_2PO_4 and 10 g of trypsin in 1 L of DI water, and the pH was adjusted to 6.8 with NaOH. The SIF was filtered by a 0.22-μm membrane before usage.

Animals

Wild-type male C57BL/6 N mice (7 weeks, SPF, purchased from SPF Beijing Biotechnology Co., Ltd.) were used in this study. For the oral administration of microbial preparations, mice were orally gavaged with 200 μl of the engineered bacterial preparation containing

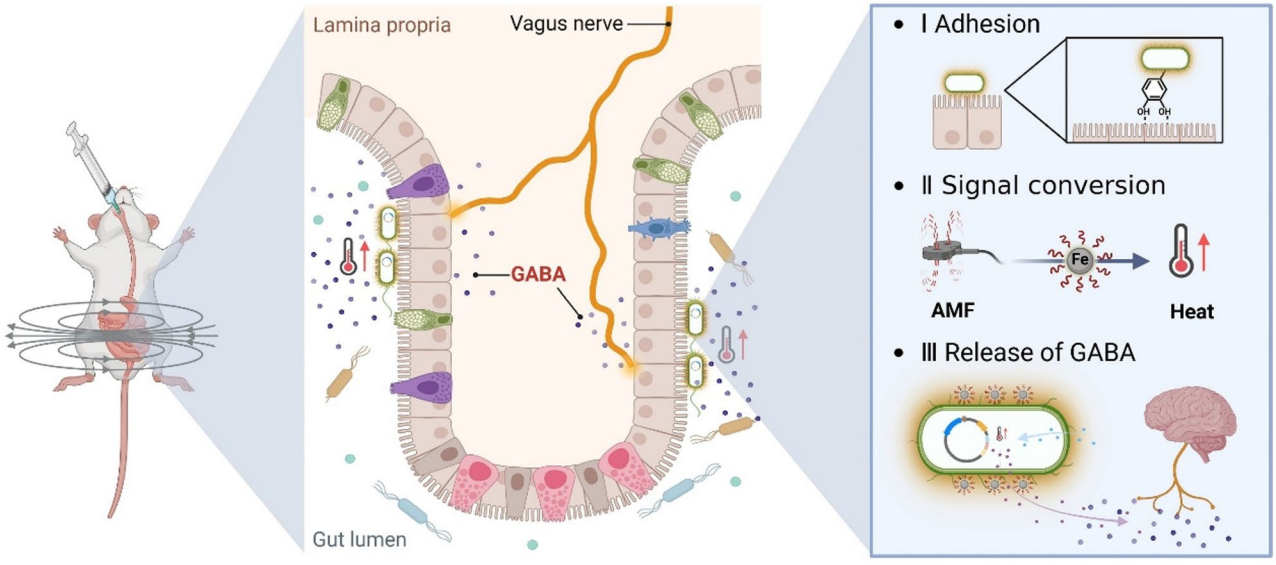

Fig. 1 Schematic illustration of EcN-GadABC@Fe-NE mechanism for regulating anxiety-like behaviors via Gut-Brain Axis

approximately 2×10^9 CFU EcN for 10 days. Additionally, all the mice were immobilized in modified plastic syringes for 2 h each day for 10 days to induce restraint stress [26]. All procedures were performed under the guidelines approved by the Institutional Animal Care and Use Committees of Jinan Microecological Biomedicine Shandong Laboratory.

Plasmid construction and bacteria engineering

The plasmid pBV220 enables the heat-induced expression of target genes when the temperature is raised to 42 °C. The genes encoding GABA synthesis and secretion (*gada*, *gadb*, and *gadc*, Table S1) were inserted into pBV220 and referred to as pBV220-GadABC (Fig. S1). This recombinant expression vector was then introduced into *Escherichia coli* Nissle 1917 (EcN), and the positive colonies were selected using kanamycin (34 μg/mL). The temperature-sensitive bacterium, referred to as EcN-GadABC, was used for subsequent modification. At the same time, the gene encoding green fluorescence protein (GFP) was also inserted into pBV220 to produce pBV220-GFP, and the visualized temperature-sensitive bacterium, EcN-GFP, was used for subsequent experiments. The primers used are listed in Table S2.

Assembly of bacteria with Fe_3O_4 NPs

According to the previous research, 13.10 g of $FeCl_3 \cdot 6H_2O$ and 6.65 g of $FeCl_2 \cdot 4H_2O$ were mixed in 80 mL of DI water. And the solution was stirred under nitrogen for 0.5 h and 45 mL of $NH_3 \cdot H_2O$ was added dropwise at 80℃. 7.5 g of citric acid in 15 mL of water was introduced after the temperature rose to 95 ℃ and stirred for 90 min. The solution was dialyzed against water with a dialysis bag (MWCO: 14 000 Da) to obtain a stable magneto fluid. Next, the magnetic nanoparticle (MNP) was modified with NH_2-PEG_{2000}-NH_2 for the surface amination. Briefly, 75 mg NH_2-PEG_{2000}-NH_2 was added to 0.5 mL MNP aqueous solution (15 mg/mL), then 8.63 mg EDC and 9.8 mg NHS were added to the solution and stirred with mechanical stirring at 25 ℃ for 3 h. The morphology of MNP was observed using Transmission Electron Microscopy (TEM).

NH_2-MNPs were linked on the surface of bacteria by amide condensation. Briefly, 1×10^{10} bacteria cells were dispersed in PBS solution, and 1 mL NH_2-MNP (1 mg/mL) was added into bacterial suspension with 1.15 mg EDC and 1.3 mg NHS. After stirring for 3 h, the modified bacteria were separated by differential centrifugation (3000 rpm, 5 min) and washed with PBS three times. The morphology of EcN- Fe_3O_4 was observed using TEM.

Encapsulation of EcN with the poly-NE layer

After washing EcN-Fe_3O_4 cells three times with PBS, norepinephrine (NE) solution (0.5 mg/mL) was added and incubated at a speed of 200 rpm for 3 h. After washing with PBS three times to remove residual NE molecules, the formed EcN-Fe_3O_4-NE cells were collected by centrifugation (3000 rpm, 5 min). The NE layer formed on the surface of bacteria was characterized by TEM. And the size and zeta potential of EcN-Fe_3O_4-NE were determined by Dynamic light scattering (DLS).

External environment resistance assay for EcN-NE

The protective effects of the NE layer on EcN against simulated GI (gastrointestinal) conditions, including SGF, SIF, and bile salts (0.4%), were measured. Briefly, for the SGF resistance assay, equal amounts of EcN, EcN-Fe_3O_4 and EcN-Fe_3O_4-NE were separately subjected to SGF and incubated at 37 °C with a shaking speed of 225 rpm. At predetermined time points, 50 μL of the sample was taken, washed with PBS, and spread on LB agar plates in sequential 10-fold dilutions. The colonies were counted after 24 h of incubation at 37 °C. To test resistance against SIF and bile salts, equal amounts of EcN, EcN-Fe_3O_4 and EcN-Fe_3O_4-NE were separately subjected to SIF and bile salts in the LB medium. At predetermined time points, the samples were collected, washed with PBS, and then resuspended in 100 μL of PBS. Next, 10 μL of CCK-8 solution was added, and the samples were incubated at 37 °C for 1 h. The OD_{450} values were recorded to evaluate the cell viability.

Evaluation of the adhesive effect of EcN-NE

EcN cells contained fluorescent reporter plasmid PAKgfpLux2 for IVIS imaging were used to monitor the distribution of engineered bacteria in mice. Briefly, the plasmid PAKgfpLux2 was electrotransformed into EcN, and the positive colonies were selected using ampicillin (100 μg/mL). To evaluate the adhesive effect of NE packaging on the intestine, the EcN- PAKgfpLux2, EcN- PAKgfpLux2@Fe, and EcN- PAKgfpLux2@Fe-NE (1×10^9 CFU, 100 μL) were incubated with freshly collected mouse intestine in PBS for 1 h and then imaged via IVIS after being washed with PBS three times. And then, a total of 9 mice (male, 7 weeks) were randomly divided into three groups ($n = 3$). The EcN- PAKgfpLux2, EcN- PAKgfpLux2@Fe, and EcN-PAKgfpLux2@Fe-NE (1×10^9 CFU, 200 μL) were orally administered in mice. At 2, 8, and 24 h, the bioluminescence of mice was detected by IVIS. In addition, the gastrointestinal tract of mice was isolated and imaged after 24 h of receiving different EcN preparations.

Alternating magnetic field treatment

To measure the magnetocaloric effect of Fe_3O_4-EcN, place the solution at the center of the induction coil to expose it to an alternating magnetic field (AMF, 310 kHz, 16.8 kA/m). The temperature of the solution was measured using a fiber optic thermometer and an infrared

thermal imager. For in vivo treatment using the AMF, mice were positioned at the center of the induction coil to receive an AMF (310 kHz, 16.8 kA/m) for 60 min. Whole-body infrared imaging of mice was performed using an infrared thermal camera (Fluke Ti400U, USA) under AMF treatment.

Functional validation of engineered bacteria in vivo

A total of 23 C57BL/6 N (male, 7 weeks) mice were used in this experiment. Mice were orally gavaged with 200 μL of the engineered bacterial preparation containing approximately 2×10^9 CFU EcN-GadABC@Fe-NE (EcN-GABA treatment, $n = 8$ mice) or EcN-GFP@Fe-NE (EcN-GFP treatment, $n = 7$ mice), and an equal amount of PBS was served as control (CTL, $n = 8$ mice) for 10 consecutive days together with the AMF stimulation (310 kHz, 16.8 kA/m). The open field test (OFT), the elevated plus maze (EPM) and the light-dark box (LDB) were used to evaluate anxiety-like behavior.

Functional validation of gastrointestinal vagal afferent

A total of 20 C57BL/6 N mice (male, 7 weeks) were used in this experiment. A total of 20 male C57BL/6 N mice (7 weeks old) were used in this experiment. To assess the involvement of gastrointestinal vagal afferents in mediating the effects of EcN-GadABC@Fe-NE under AMF stimulation, we employed a chemogenetic strategy using Designer Receptors Exclusively Activated by Designer Drugs (DREADDs) to counteract GABA-mediated inhibition selectively. Mice were co-injected with two types of viral vectors: A retrograde adeno-associated virus (AAVrg) encoding Cre recombinase was injected into the wall of the stomach and intestine (0.3 μL per site, 10–20 sites per mouse); A Cre-dependent excitatory DREADD vector (AAV2/9-DIO-hM3D-mCherry, 0.5 μL) was injected into the right nodose ganglion, where the somata of gastrointestinal vagal sensory neurons reside. Upon administration of clozapine-N-oxide (CNO, 1 mg/k), the targeted vagal afferent neurons were selectively activated, thereby counteracting the inhibitory effect of GABA produced by EcN-GadABC@Fe-NE under AMF exposure. All mice underwent viral injections and were randomly divided into three treatment groups: CTL group (gavage of 200 μL PBS, $n = 7$), EcN-GABA group (gavage of 200 μL EcN-GadABC@Fe-NE, $n = 6$), EcN-GABA + CNO group (gavage of 200 μL EcN-GadABC@Fe-NE preparation plus CNO injection, $n = 7$).

Open field test (OPT)

A single mouse was placed in the center of the OPT chamber ($60 \times 60 \times 50$ cm), the region of which was divided into nine equal parts. The mice were allowed to move freely in the box for 3 min. The time spent in the center zone and total moving distance were calculated to evaluate the anxiety level of mice.

Elevated plus maze (EPM)

A single mouse was placed in the center of the EPM chamber ($30 \times 5 \times 15$ cm) with its head facing the open arm. The mouse's movement in the EPM was recorded for 3 min. The entry ratio and time spent in the open arm were calculated to assess the anxiety level of the mice.

Light-Dark box (LDB)

The LDB box ($44 \times 21 \times 21$ cm) was divided into two equal compartments (light chamber and dark chamber) by a partition (1 cm) with a small aperture (5×7 cm) in the center, allowing the mice to move freely between the light and dark chambers. A single mouse was placed in the dark chamber facing the end wall and allowed to move freely in the box for 5 min. The latency to go to the light chamber and residence time in each chamber were calculated to evaluate the anxiety level of the mice.

Intestinal microbiota analysis

After treating mice with engineered bacteria by gavage for 10 days, feces were collected and immediately frozen in liquid nitrogen, and intestinal microbiome analysis was performed by 16 S rRNA sequencing analysis. Briefly, the total DNA was extracted using the CTAB according to manufacturer's instructions, and the extracts were measured on 1% agarose gel. The V3-V4 region of the bacterial 16 S rRNA gene was amplified using the barcoded primer sets 338 F (5′-ACTCCTACGGGAGGCAGCAG-3′) and 806R (5′-GGACTACHVGGGTWTCTAAT-3′). The PCR products were purified by AMPure XT beads (Beckman Coulter Genomics, Danvers, MA, USA) and quantified by Qubit (Invitrogen, USA). The amplicon pools were prepared for sequencing and the size and quantity of the amplicon library were assessed on Agilent 2100 Bioanalyzer (Agilent, USA) and with the Library Quantification Kit for Illumina (Kapa Biosciences, Woburn, MA, USA), respectively. The libraries were sequenced on Illumina NovaSeq PE250 platform at LC-Biotechnology Co., Ltd (Hangzhou, China). Paired-end reads were merged using FLASH. Quality filtering on the raw reads was performed under specific filtering conditions to obtain high-quality clean tags according to the fqtrim (v0.94). Chimeric sequences were filtered using Vsearch software (v2.3.4). After dereplication using DADA2, the feature table and feature sequence were obtained.

Statistical analysis

Statistical analysis was conducted using GraphPad Prism 10.1.2. The statistical significance was determined using Student's t-test and one-way ANOVA (analysis of

variance) followed by Tukey's least significant difference multiple comparisons. The differences between experimental and control groups were considered statistically significant at the following *p*-values: n.s. (not significant) $p > 0.05$, $^{*}p < 0.05$, $^{**}p < 0.01$, $^{***}p < 0.001$, $^{****}p < 0.0001$.

Results

Construction and characterization of the thermal-sensitive probiotic

To achieve temperature-actuated release of gamma-aminobutyric acid (GABA), we modified the probiotic *Escherichia coli* Nissle 1917 (EcN) to express the three crucial genes *gada/b/c* involved in bacterial GABA production under the control of temperature-responsive promoter pRpL. The genes *gada/b* encode the glutamate decarboxylase, which catalyzes the conversion of glutamate (Glu) to GABA, and the gene *gadc* encodes Glu-GABA antagonistic transporter, which bidirectional transports GABA and Glu (Fig. 2A). Regulated by the inhibitor CITs protein, the pRpL promoter is inhibited at 37 °C and disinhibited at 42 °C, leading to targeted gene transcription (Fig. 2B). We first transfected the EcN with the plasmid (pBV220-pRpL-GFP) containing green fluorescent protein (GFP) as the reporter gene to generate EcN-GFP. The GFP intensity increased with the increase of culture temperature (Fig. 2C and D), and the OD_{600}-normalized fluorescence of EcN-GFP elevated as the temperature of the culture increased (Fig. 2E). These data confirmed the time and temperature dependency of the EcN containing plasmid pBV220-pRpL. Subsequently, plasmid pBV220-pRpL-GadABC containing the genes *gada*, *gadb* and *gadc* was transformed into EcN to obtain EcN-GadABC. Using real-time PCR, we confirmed the expression levels of genes *gada*, *gadb* and *gadc* in EcN-GadABC. The expression of three genes was significantly increased in EcN-GadABC when the culture temperature rose from 37℃ to 42℃, while the expression levels remained unchanged in wild-type EcN (Fig. 2F). In addition, we found that the concentration of GABA produced by EcN-GadABC was significantly higher than that of wild-type EcN after culturing at 42 ℃ for 1 h and 2 h (Fig. 2G). Together, these results indicated that the engineered probiotic EcN-GadABC was capable of releasing GABA under temperature control.

Assembly of the thermal switch to the EcN-GadABC

To acquire accurate temporal control of temperature, NH_2-Fe_3O_4 nanoparticles (NPs) were assembled to the surface of EcN-GadABC as the thermal switch through amide condensation reaction. The amino group of NH_2-Fe_3O_4 reacts with the carboxyl group of N-acetyl muramic acid located at the outer membrane of the bacterial cell wall under the catalyzation of EDC and NHS (Fig. 3A). Transmission electron microscopy (TEM) images showed that Fe_3O_4 was successfully anchored to the surface of the bacteria and formed EcN-GadABC@Fe_3O_4 (EcN-GadABC@Fe) (Fig. 3B). The temperature of the EcN-GadABC@Fe suspension was significantly elevated by 5–7 ℃ upon the AMF stimulation (310 kHz and 16.8 kA/m) (Fig. 3C and D), which confirmed the magneto-thermal converting capacity of EcN-GadABC@Fe. Meanwhile, the temperature change of the EcN-GadABC@Fe suspension remained stable during the six cycles of AMF stimulation and cooling at room temperature (Fig. 3E), suggesting the stability of the magnetic-thermal conversion. Using the reporter EcN (EcN-GFP@Fe), we further confirmed that AMF stimulation induced a significant increase in fluorescent intensity after 60 min (Fig. 3F, G). And the concentration of GABA produced by EcN-GadABC@Fe was significantly higher after 1 h with AMF stimulation (Fig. 3H). In addition, whole-body infrared imaging revealed that the temperature of the intestine was elevated with AMF stimulation (Fig. 3I). These results together proved that the Fe_3O_4 NPs on the engineered probiotic were able to receive and convert magnetic signals to thermal signals stably, thereby acting as an efficient thermal switch.

Encapsulation of protective and adhesive layer to EcN-GadABC@Fe

The harsh environmental conditions in the GI tract prevent colonization and prolonged survival of exogenous probiotics [27, 28]. Poly-norepinephrine (poly-NE) is the oxidative polymerization of norepinephrine, which forms a nearly perfect smooth surface and is capable of storing and releasing small therapeutics [29]. We then encapsulated the EcN-GadABC@Fe with poly-NE to obtain EcN-GadABC@Fe-NE (Fig. 4A). The TEM image clearly showed the smooth and transparent layer of the poly-NE coating (Fig. 4B). The size of the EcN increased from 1231 nm to 1576 nm, and the zeta potential rose from − 24.7 MV to -11.9 MV (Fig. 4C) after encapsulation, indicating the presence of poly-NE layer on the surface of EcN. The assembly of Fe_3O_4 and poly-NE layers on the surface of EcN did not adversely affect its growth (Fig. 4D). Next, we examined whether the poly-NE layer could protect the EcN against gastric-environmental assaults. When treated with simulated gastric fluid (SGF) to mimic the acidic gastric environment in the stomach, the viability of EcN-GadABC@Fe-NE was significantly higher than that of EcN-GadABC and EcN-GadABC@Fe after 0.5, 1 and 2 h of incubation (Fig. 4E). The EcN-GadABC@Fe-NE also showed a higher survival rate when subjected to simulated intestinal fluid (SIF) and bile salt (Fig. 4F and G). These results together confirmed the application of poly-NE as a protective coating layer for orally administered probiotics.

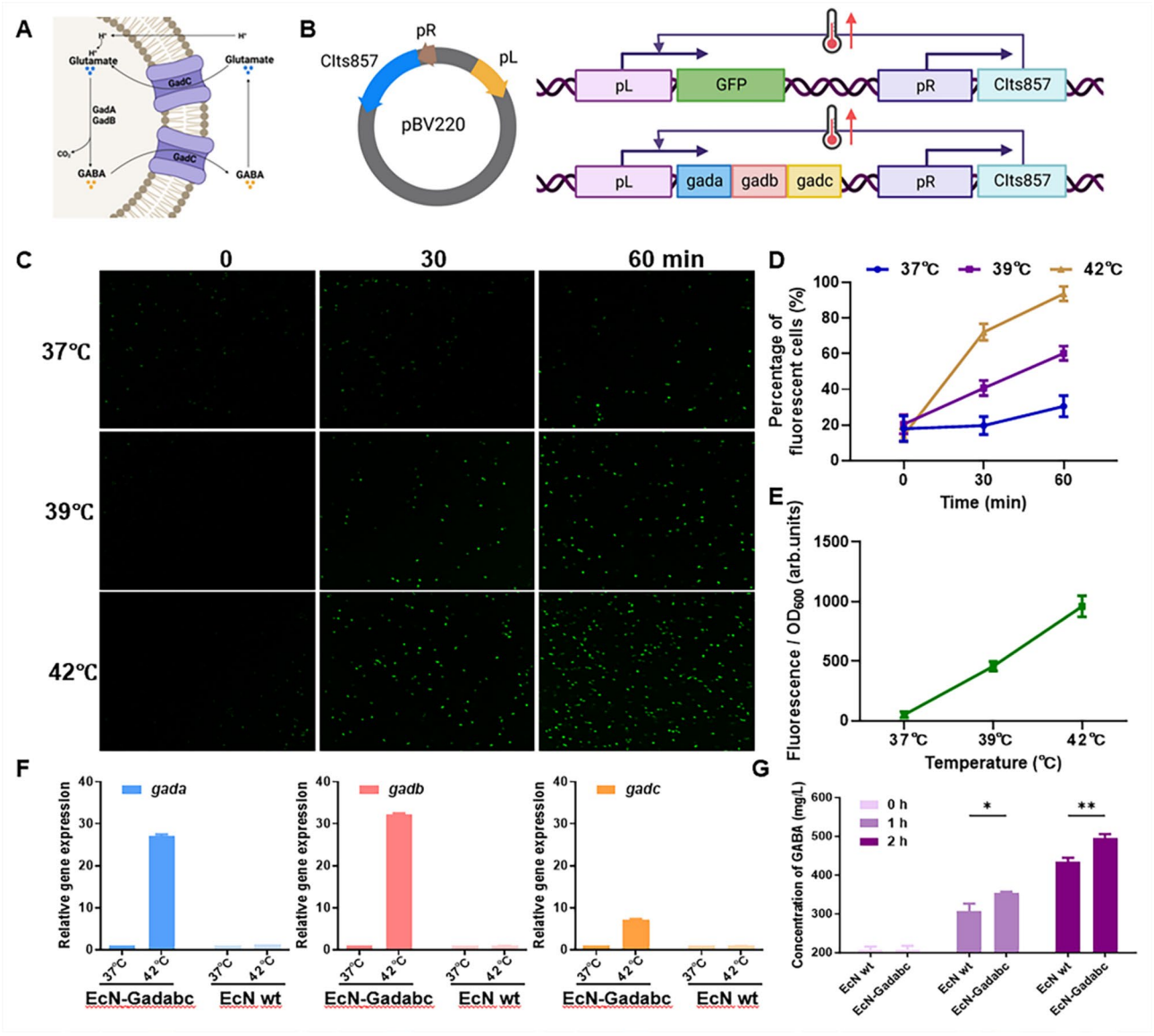

Fig. 2 Design and construction of temperature-sensitive bacterium EcN-GadABC. (**A**) Three genes involved in GABA production by *E. coli*. *gadA*: glutamate decarboxylase A; *gadB*: glutamate decarboxylase B; *gadC*: Glu-GABA antagonistic transporter. (**B**) The schematic diagram of plasmid pBV220 and the pRpL promoter responding to temperature changes in EcN. (**C**) Fluorescent images of EcN-GFP with the temperature rise. Scale bar, 10 μm. (**D**) Percentage of fluorescent cells after being cultured at 37 °C, 39 °C, and 42 °C for 30 and 60 min. (**E**) Optical density (OD_{600})-normalized fluorescence of EcN-GFP cultured at 37 °C, 39 °C, and 42 °C for 60 min. (**F**) Relative gene expression of *gadA*, *gadB*, and *gadC* in EcN-GadABC and wildtype EcN cultured under 37℃ and 42℃. (**G**) The concentration of GABA in the supernatant in wildtype EcN and EcN-GadABC cultured at 42℃. Data are presented as means ± SEM ($n = 3$). Statistical analysis was performed using t-test. *$p < 0.05$, **$p < 0.01$, ***$p < 0.001$

We monitored the distribution of engineered bacteria through bioluminescence signals via IVIS to further investigate whether the poly-NE coating can increase the mucosal adhesion and prolong the survival of the engineered probiotics. As shown in Fig. 4H and G, the fluorescence intensity of collected mouse intestines with the EcN@Fe-NE was much higher than that with EcN and EcN@Fe, demonstrating the improved adhesive capability of the EcN to the intestinal mucosa. Because of the robust mucoadhesive capability of the NE layer observed ex vivo, we next examined the intestinal retention time of EcN, EcN@ EcN@Fe, and EcN@Fe-NE in vivo. As shown in Fig. 4J and K, the EcN@Fe-NE exhibited prolonged retention time in the intestine of host mice when compared to the EcN and EcN@Fe. The bioluminescence intensity of the EcN@Fe-NE group was significantly higher than that of the EcN and EcN@Fe groups at 8 h and 24 h as evidenced by a slower rate of bioluminescent signal decay in the EcN@Fe-NE group. After 24 h, the mice were euthanized, and the intestines were collected

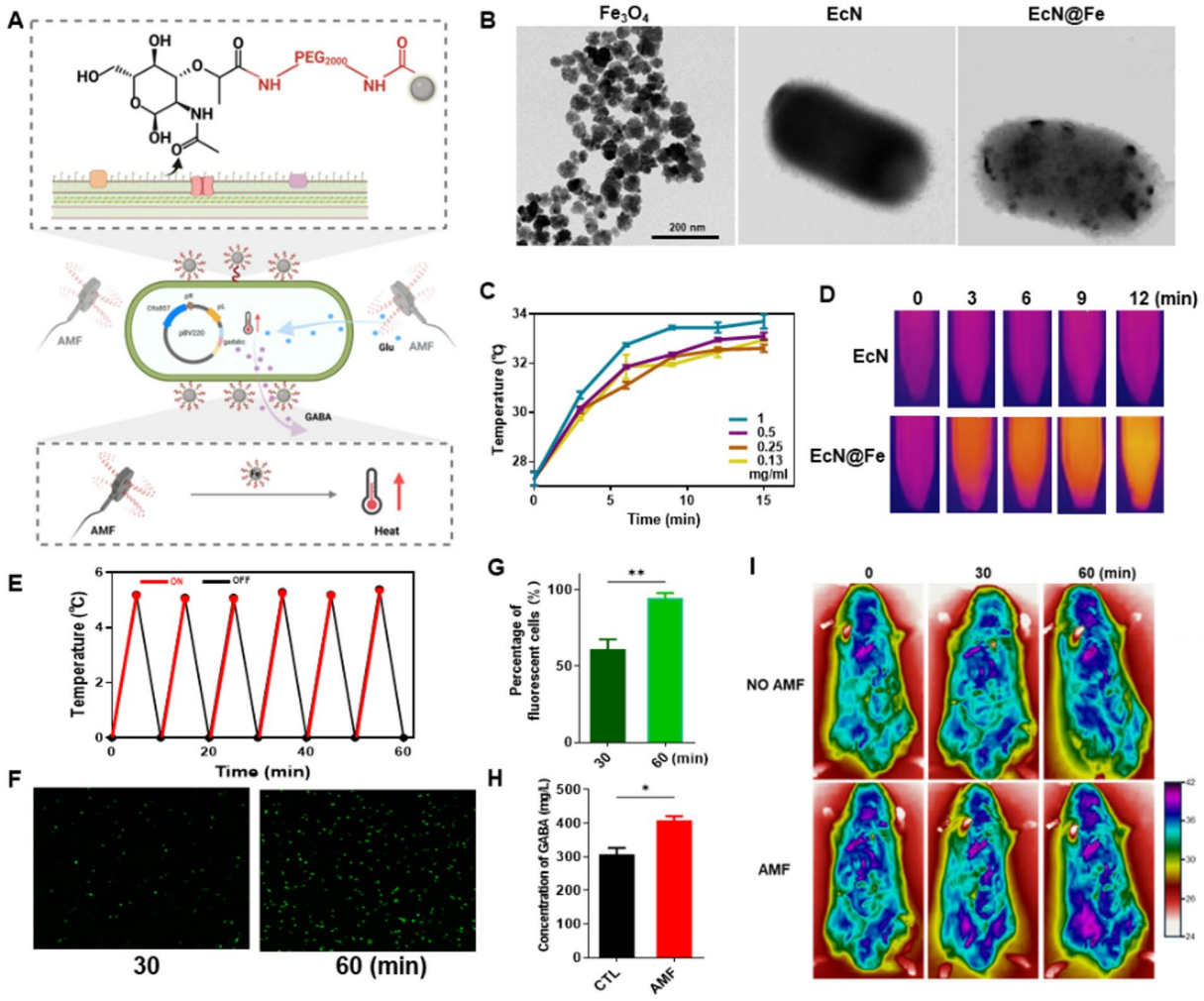

Fig. 3 Assembly of Fe_3O_4 NPs to the EcN-GadABC. (**A**) The schematic diagram of the mechanism of Fe_3O_4 NPs connected to the surface of bacteria. (**B**) The TEM images of Fe_3O_4 NPs, EcN, and EcN@Fe. Scale bar, 200 nm and 0.5 μm. (**C**) The temperature changes of EcN@Fe solutions with different concentrations of Fe_3O_4 assembled to bacteria under AMF stimulation. (**D**) Infrared images of EcN solution and EcN@Fe solution under AMF stimulation for 12 min. (**E**) The temperature changes of EcN@Fe solutions during six cycles of AMF stimulation and natural cooling-down. (**F**) Fluorescent images of EcN-GFP@Fe under AMF stimulation for 30 and 60 min. Scale bar, 10 μm. (**G**) Percentage of fluorescent cells after being treated with AMF stimulation for 30 and 60 min. (**H**) The concentration of GABA secreted by EcN-GadABC@Fe with or without AMF stimulation. (**I**) Infrared imaging of mice treated with EcN-GadABC@Fe/AMF. Data are presented as means ± SEM ($n = 3$). Statistical analysis was performed using t-test. *$p < 0.05$, **$p < 0.01$, ***$p < 0.001$

for ex vivo IVIS imaging. As shown in 4 L and 4 M, the bioluminescence intensity of EcN@Fe-NE was significantly higher than that of the EcN and EcN@Fe groups, respectively, which demonstrated the enhanced mucoadhesive capability of bacteria endowed by the NE layer coating.

Alleviation of anxiety-like behaviors by EcN-Gadabc@Fe-NE

To verify the effects of EcN-GadABC@Fe-NE in relieving anxiety-like behaviors in vivo, we gavaged the mice with EcN-GadABC@Fe-NE, EcN-GFP@Fe-NE, and an equal amount of PBS for 10 days together with the AMF stimulation (Fig. 5A). In the open field test (OFT), the mice treated with the EcN-GadABC@Fe-NE/AMF (EcN-GABA group) exhibited a trend of increase in time spent in the center zone when compared with mice treated with the EcN-GFP@Fe-NE/AMF (EcN-GFP group) (Fig. 5B), indicating that the engineered probiotics prevented the open-field-induced anxiety. In the EPM test, the EcN-GABA mice showed a significant increase in the time spent in the open arm compared with that of the other two groups (Fig. 5C), further confirming the anxiolytic effects of the engineered probiotics on height-induced anxiety. Moreover, when tested in LDB, the EcN-GABA mice also showed shorter latency in the dark box, increased entry numbers of the light box and longer stay in the light box compared with EcN-GFP mice (Fig. 5D). Besides, the concentration of GABA in the serum of mice treated with EcN-GadABC@Fe-NE/AMF was

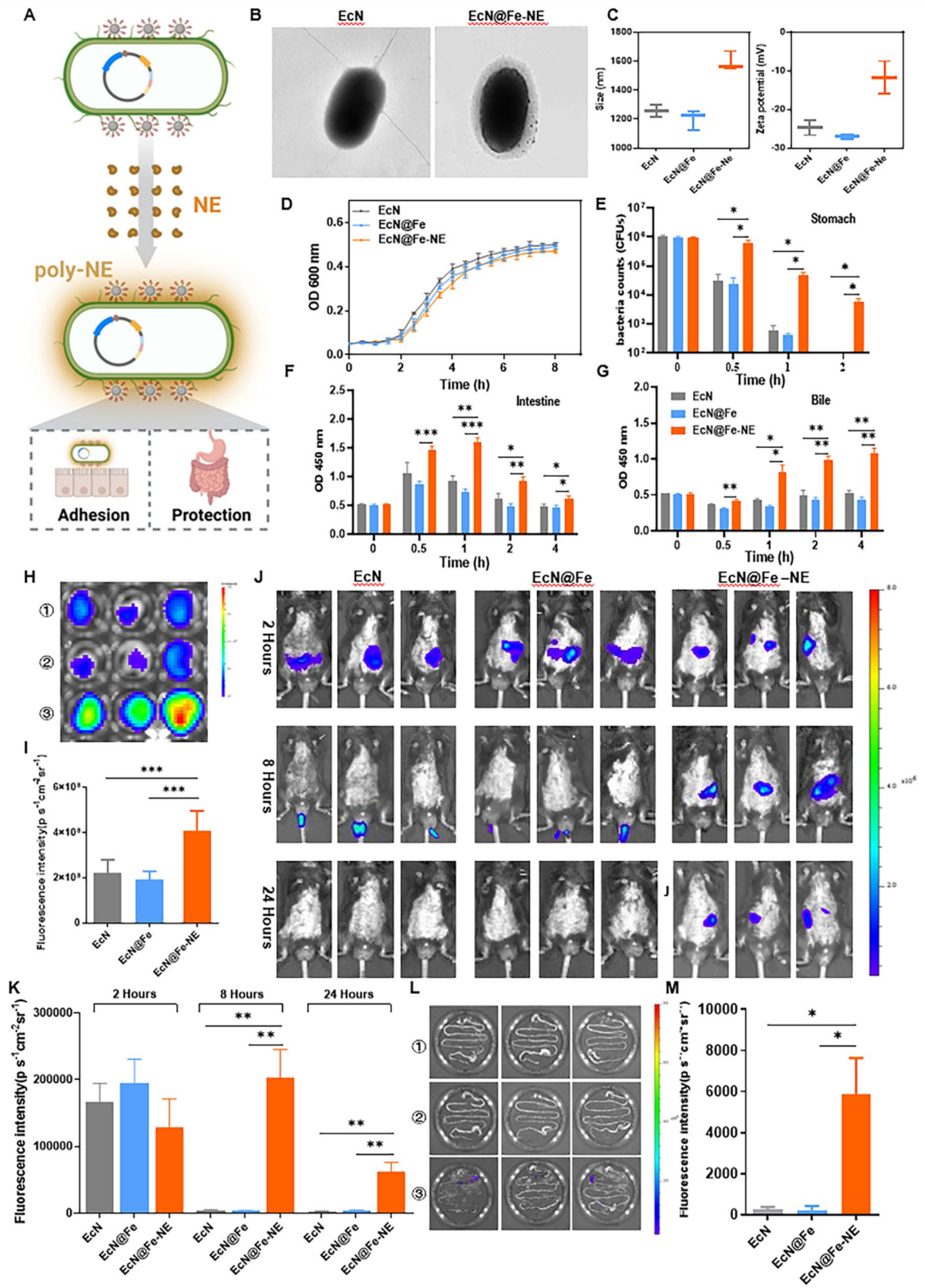

Fig. 4 (See legend on next page.)

(See figure on previous page.)

Fig. 4 Assembly of the protective and adhesive layer to the EcN-GadABC@Fe. (**A**) The schematic diagram of the poly-NE assembly process and function. (**B**) TEM images of EcN and EcN@Fe-NE. Scale bar, 0.5 μm. (**C**) The sizes and zeta potentials of EcN, EcN@Fe, and EcN@Fe-NE. (**D**) The growth curve of EcN, EcN@Fe, and EcN@Fe-NE. (**E-G**) Survival of EcN, EcN@Fe, and EcN@Fe-NE after exposure to the SGF, SIF, and bile salt. CFU, colony forming units. (**H**) Bioluminescence images of ex vivo intestines after incubation with EcN (①), EcN@Fe (②), and EcN@Fe-NE (③). (**I**) Region-of-interest analysis of fluorescence intensities of the intestines. (**J**) Bioluminescence images of the mice orally gavaged with EcN, EcN@Fe, and EcN@Fe-NE at different time points. (**K**) Region-of-interest analysis of bioluminescence intensities of the mice orally gavaged with EcN, EcN@Fe, and EcN@Fe-NE at different time points. (**L**) Bioluminescence images of mice GI tracts after orally gavaged with EcN (①), EcN@Fe (②), and EcN@Fe-NE (③) for 24 h. (**M**) Region-of-interest analysis of bioluminescence intensities of the GI tracts after orally gavaged with EcN, EcN@Fe, and EcN@Fe-NE for 24 h. Data are presented as means ± SEM ($n = 3$). Statistical analysis was performed using one-way ANOVA. *$p < 0.05$, **$p < 0.01$, *** $p < 0.001$

significantly higher than that without AMF treatment (Fig. S2). These results showed that the EcN-GadABC@Fe-NE together with AMF stimulation exhibited general and significant anxiolytic efficacy in the mouse model of acute anxiety.

In correlation with the behavioral observations, we also examined the changes in the activity of brain regions that are closely involved in regulating anxiety-like behaviors. We noticed that the activation of NTS regions was indeed inhibited by the EcN-GABA treatment in comparison with that of mice in the EcN-GFP group (Fig. 5E). More importantly, a significant reduction in the activity of the LC region, particularly the NE neurons in the LC was observed in the EcN-GABA mice (Fig. 5F), suggesting an inhibition of the anxiogenic hub area. In addition, we also observed general activity changes in multiple brain regions involved in modulating mood and anxiety, including the central amygdala, the lateral habenula, and the infralimbic cortex, etc. (Fig. S3).

Anxiolytic effects through inhibiting Gastrointestinal vagal afferent

The neurotransmitter GABA crosses the blood-brain barrier in minuscule amounts [30, 31], therefore, GABA released in the gut is more likely to influence brain function through indirect pathways. As shown in Fig. 6A and B, the chemogenetic counteraction of vagal sensory inhibition successfully attenuated the anxiolytic effects of EcN-GadABC@Fe-NE/AMF treatment, reducing both the time spent in the center in the OFT (Fig. 6C) and the time spent in the open arm in the EPM (Fig. 6D). Similarly, compared to mice that were treated with EcN-GadABC@Fe-NE/AMF and saline, counteracting vagal inhibition significantly reduced the number of entries and the time spent in the light box, indicating the blockade of anxiolytic effects of EcN-GadABC@Fe-NE/AMF treatment (Fig. 6E). Since the GABA receptors (gabbr1/2) are highly expressed at the terminal of vagal sensory neurons innervating the stomach and intestine [20], a selective $GABA_B$ receptor antagonist CGP35348 was used by oral gavage to test whether the released GABA by the EcN exert anxiolytic effects through the vagal sensory input. Pretreatment of the CGP35348 partially attenuated the anxiolytic effects of GABA (Fig. S4), indicating a $GABA_B$ receptor-mediated mechanism. These results together suggested that the anxiolytic effects of EcN-GadABC@Fe-NE/AMF were largely mediated through inactivation of the gastrointestinal vagal afferents.

Modulation of gut microbiota by EcN-GadABC@Fe-NE

Since probiotics can modulate gut microbiota and exert beneficial effects on the host, we analyzed the diversity and composition of the gut microbiota of EcN-GadABC@Fe-NE /AMF treated mice. The Shannon, ACE and Pielou indexes were analyzed to assess the α diversity of gut microbiota, and the results indicated that the EcN-GadABC@Fe-NE/AMF treatment would restore the reduction in the diversity of gut microbiota in the EcN-GFP@Fe-NE/AMF treated mice (Fig. 7A). At the same time, the β diversity of microbial communities in the gut under different treatments was analyzed, and PCA revealed that the first two axes explained 90.49% of the variance between samples (Fig. 7B), indicating that the bacterial community structure was significantly shaped by foreign bacterium (Adonis, $p < 0.05$).

All ASVs were annotated from the phylum to the genus level. The dominant genera in the three treatments are presented in Fig. 7C. The gavage of EcN, regardless of EcN-GadABC@Fe-NE or EcN-GFP@Fe-NE, significantly changed the composition of gut microbiota in mice. Specifically, the relative abundances of *Ligilactobacillus* and *Lactobacillus* in the ECN gavage treatment group increased and became the dominant genera, which were significantly more abundant than that in the CTL treatment (Fig. 7D). Furthermore, the relative abundances of *Alistipes* and *Desulfovibrio* were significantly decreased with ECN gavage. Biomarker analysis using the LEfSe method showed significant differences in the microbial community components of the three treatments from the phylum to genus levels ($p < 0.05$). As shown in Fig. 7E and S5, 92 bacterial clades presented statistically significant differences with an LDA threshold of 3.0 between CTL, EcN-GFP@Fe-NE, and EcN-GadABC@Fe-NE groups, indicating that the foreign bacterium had a significant impact on the level of classification from the phylum to genus levels. To test whether the anxiolytic effects of the EcN-GadABC@Fe-NE/AMF was mediated by the gut microbiota, mice were pretreated with antibiotic (ABX) to deplete the gut microbiota. We found that certain behavioral improvements, for example, the increased

frequency to the lightbox in the LDB test, was abolished in ABX mice, while other anxiolytic effects, such as increased frequency and the time spent in the open arm in the EPM test, were unaffected (Fig. S6). These results indicated that the anxiolytic effects of EcN-GadABC@Fe-NE/AMF were mediated through both modulation of anxiety-related neural networks and the maintenance of gut microbiota homeostasis.

Discussion

As the direct neural path connecting the gastrointestinal tract and the brain, the vagus nerve is the key component of the gut-brain axis. The gastrointestinal innervating vagal afferents are crucially involved in directly modulating and mediating the regulatory effects of the gut microbiome on mood and anxiety [31]. Naturally and preferably colonized in the gastrointestinal tract, the probiotics are ideally suited for gut-brain axis modulation. In addition, with the advantages of flexible design, controllable release, and targeted delivery, genetically engineered bacteria have been designed to serve as powerful drug factories to produce and deliver a series of bioactive molecules for therapeutic purposes [32, 33]. Therefore, in this study, we have constructed and tested a nanomaterial-assisted engineered bacteria system to controllably release the gamma-aminobutyric acid (GABA) upon the alternative magnetic field (AMF) stimulation to silence the gastrointestinal vagal afferent and to relieve anxiety-like behaviors. Using probiotic *E. coli* Nissle 1917 as the chassis bacteria, we showed that the nanomaterial-assisted engineered bacteria system EcN-GadABC@Fe-NE, utilized together with the AMF, was able to reduce anxiety levels in mice through inhibition of gastrointestinal vagal afferents and restoration of gut microbiota dysbiosis.

Although naturally suited for in vivo gut-brain axis regulation, the engineered probiotics require more precise control to achieve reliable dose-response relationships and strict temporal regulation. Various sensing modules have been applied to the engineered probiotics to achieve precise temporal control in vivo. For example, Pan et al. have reported an upconversion optogenetic micro – nano system to effectively regulate the gut-brain axis [34]. In addition to optogenetic signals, biological sensors responsive to tetrathionate [35], bile acid [36], and thermal signals [37] have also been used as control strategies. Among them, thermal control shows unique advantages, allowing multiple relatively simple ways of conversion and considerable temporal accuracy. Herein, we combined the magnetic nanoparticle Fe_3O_4 with AMF to convert thermal signals as control strategies. Taking advantage of the superior tissue penetration, the non-invasiveness, and the temporal-spatial accuracy of AMF [38], the EcN@Fe exhibited effective time- and field-strength-dependent thermal conversion, enabling controlled release of GABA in vivo.

The oral administration of exogenous engineered bacteria displays inevitable problems of low bioavailability and limited intestinal colonization due to environmental assaults in the gastrointestinal tract. Surface modifications with nanomaterials provide useful strategies to protect living probiotics from external environmental assaults and provide extra characteristics necessary to achieve successful treatment efficacy, such as reduced immunogenicity, enhanced muco-adhesion, targeted delivery, in vivo visualization, etc [39]. For example, the encapsulation of the probiotics with biocompatible lipids significantly improved the survival of bacteria against various extreme conditions without affecting their viability and bioactivity [40]. Through LbL self-assembly, Anselmo et al. reported encapsulating probiotics with polysaccharides to protect the probiotics from GI tract insults and facilitate bacterial muco-adhesion [41]. The norepinephrine (NE) can form a poly-NE coating layer when auto-oxidized [29], yielding a relatively smooth nanoscale surface at the nanoscale and simultaneously serving as a reservoir for the controlled release of small therapeutic molecules [29]. Encapsulating the EcN@Fe with Poly-NE, we constructed the EcN-GadABC@Fe-NE, and the poly-NE coating significantly enhanced the survival of the probiotics against acidic gastric fluid, digestive enzymes, and bile salts. In addition, the poly-NE encapsulation also enhanced the muco-adhesion of EcN-GadABC@Fe-NE. Compared to the uncoated probiotics, the EcN-GadABC@Fe-NE showed a significantly higher *in vivo and in vitro* fluorescent signal at 24 h after oral administration, indicating enhancement of muco-adhesion.

The gastrointestinal innervating vagal afferents mediate pathogenic bacteria-induced anxiety-like behaviors [42]. Interestingly, chemogenetic inhibition of gastric-innervating vagal afferents exhibits significant anxiolytic effects [43]. The vagal afferents connect with several key brain regions involved in mood regulation, including the hypothalamus, the locus coeruleus (LC), and the ventral tegmental area through the nucleus of the solitary tract (NTS). As an integrating center for sensory, visceral, and somatic information [44, 45], the NTS directly modulates the HPA axis activity mainly through noradrenergic and adrenergic projections to the PVN [44], indicating its important role in stress pathways. Similar to the above findings, we show that EcN-GadABC@Fe-NE/AMF significantly reduces the restraint-induced activation of NTS, which could underlie its anxiolytic effects. More importantly, the prevention of gastrointestinal vagal afferents inhibition abolished the anxiolytic effects of EcN-GadABC@Fe-NE/AMF further demonstrating that the inhibition of NTS through reducing the

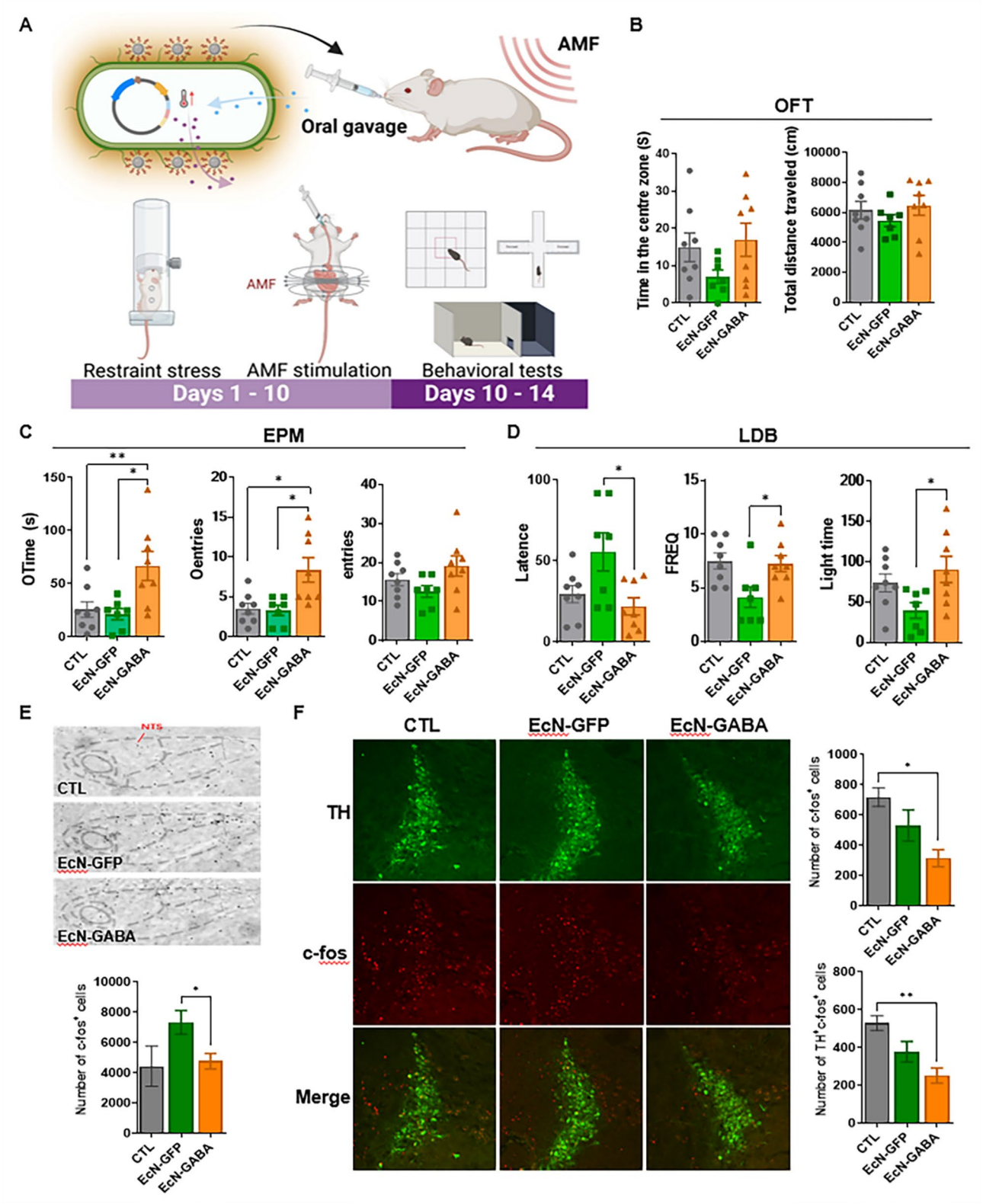

Fig. 5 (See legend on next page.)

(See figure on previous page.)

Fig. 5 Determination of in vivo function of EcN-GadABC@Fe-NE in mice. (**A**) The schematic diagram of experimental design. (**B**) Total distance traveled and time in the center zone of the open field test (OFT) from the CTL, EcN-GFP, and EcN-GABA groups. (**C**) Summarized data of the time stay in the open arms, the number of open arms entries and the number of total entries of the elevated plus maze (EPM) from the CTL, EcN-GFP, and EcN-GABA groups. (**D**) Summarized data of latency in the dark chamber, number of entries to the light chamber and time stay in the light chamber of the light-dark box (LDB) from the CTL, EcN-GFP, and EcN-GABA groups. CTL: $n = 8$ mice, EcN-GFP: $n = 7$ mice, EcN-GABA: $n = 8$ mice. (**E**) Immunohistochemical images and quantitative analysis of c-Fos–labeled cells within the nucleus of the solitary tract (NTS) in CTL, EcN-GFP, and EcN-GABA groups after 10 days of treatment. (**F**) Immunofluorescence images and quantitative analysis of c-Fos–labeled and c-Fos + tyrosine hydroxylase (TH) – labeled cells within the locus coeruleus (LC) in CTL, EcN-GFP and EcN-GABA groups after 10 days of treatment. Scale bar: 100 μm. All data are presented as mean ± SEM. Statistical analysis was performed using one-way ANOVA. $^{*}p < 0.05$, $^{**}p < 0.01$, $^{***}p < 0.001$

gastrointestinal vagal activation contributed to the anxiolytic effects of EcN-GadABC@Fe-NE/AMF. Furthermore, pretreatment with the $GABA_B$ receptor antagonist through gavage partially blocked the anxiolytic effects of orally administered GABA. Since only a limited amount of GABA in the periphery can cross the blood–brain barrier, and $GABA_B$ receptors are highly expressed on vagal sensory neurons [20], we suspect that the anxiolytic effects of EcN-GadABC@Fe-NE are possibly mediated through the $GABA_B$ receptors at the terminals of vagal afferents.

Vagal afferent inputs terminate in the nucleus of the solitary tract (NTS), and NTS is directly connected with multiple brain regions that are closely related to anxiety-like behaviors, such as the LC, VTA, BNST (bed nucleus of the stria terminalis), etc [46]. We noticed a significant

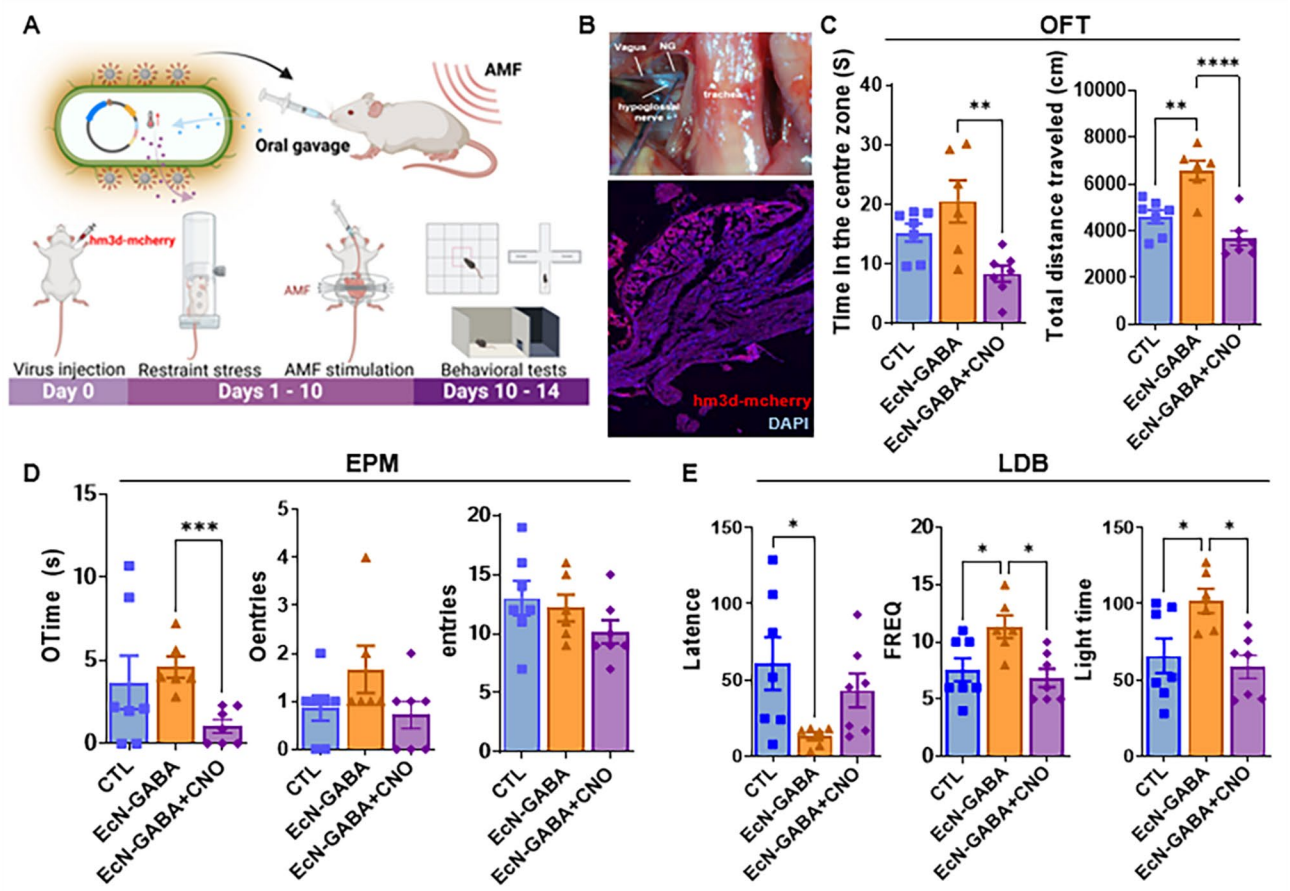

Fig. 6 Verification of EcN-GadABC@Fe-NE worked through the vagus nerve. (**A**) The schematic diagram of experimental design. (**B**) Expression of hm3d-mcherry in the vagus nerve. (**C**) Total distance traveled and time in the center zone of the open field test (OFT) from the CTL, EcN-GABA, and EcN-GABA + CNO groups. (**D**) Summarized data of the time stay in the open arms, the number of open arms entries and the number of total entries of the elevated plus maze (EPM) from the CTL, EcN-GABA, and EcN-GABA + CNO groups. (**E**) Summarized data of latency in the dark chamber, number of entries to the light chamber and time stay in the light chamber of the light dark box (LDB) from the CTL, EcN-GABA, and EcN-GABA + CNO groups. CTL: $n = 7$ mice, EcN-GABA: $n = 6$ mice, EcN-GABA + CNO: $n = 7$ mice. All data are presented as mean ± SEM. Statistical analysis was performed using one-way ANOVA. $^{*}p < 0.05$, $^{**}p < 0.01$, $^{***}p < 0.001$, $^{****}p < 0.0001$

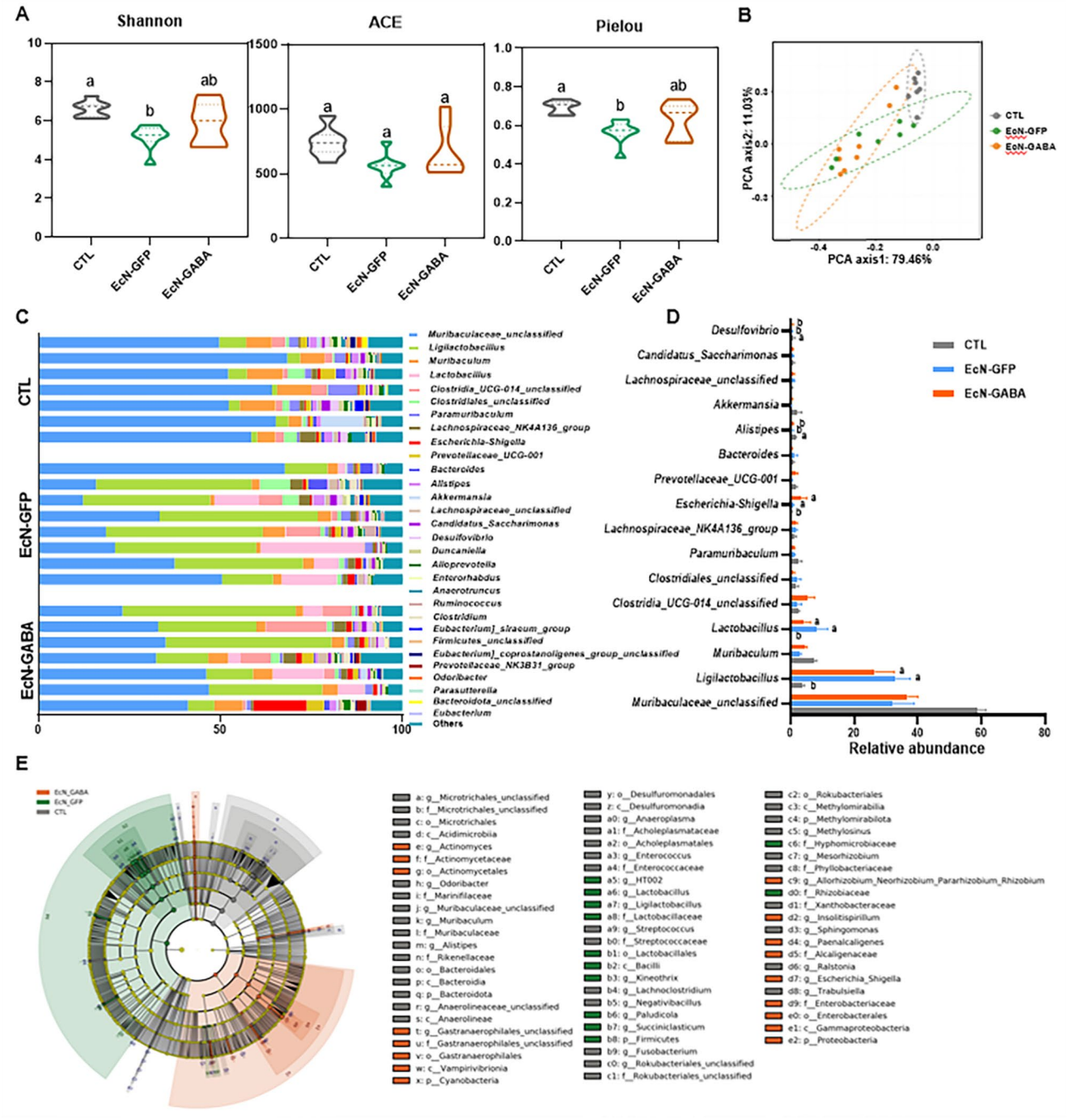

Fig. 7 Changes in gut microbiota after EcN@Fe-NE/AMF treatment. (**A**) The α diversity (Shannon, pielou, and ACE indices) of gut microbiota at 10 d. (**B**) The β diversity (principal component analysis, PCA) of gut microbiota at 10 d. Dots displaying low separation indicate similar community structures, and vice versa. The dotted circle represents the 95% confidence interval. (**C**) Relative abundance of gut microbiota at the genus level in the CTL, EcN-GFP, and EcN-GABA groups at 10 d. (**D**) Relative abundance of the Top 16 genera in the CTL, EcN-GFP, and EcN-GABA groups at 10 d. (**E**) LEfSe analysis of microbial abundance between CTL, EcN-GFP, and EcN-GABA groups. The different and same letters indicate significant ($p < 0.05$) and nonsignificant ($p > 0.05$) differences, respectively

inhibition of LC activity after the EcN-GadABC@Fe-NE/AMF treatment, particularly a reduced activation of the norepinephrine (NE) neurons in the LC, which could possibly explain the anxiolytic effects of the engineered bacteria we observed in restraint mice. The LC-NE neurons showed increased activity during restraint stress, and suppression of LC-NE neurons can alleviate the restraint-stress-induced anxiety-like behaviors [47]. Furthermore, considerable evidence from human and animal studies also illustrated the general involvement

of increased LC-NE neuron activity in the development of pathological anxiety [48–51] and the anxiolytic effects of LC lesion or LC-NE neuron inhibition [51–53]. Therefore, we believe that suppression of LC-NE neurons through the vagal inhibition of NTS could be the neural mechanism underlying the anxiolytic effects of EcN-GadABC@Fe-NE/AMF treatment.

The onset of anxiety is also closely related to the imbalance of gut microbiota [54]. Taking advantage of the capability of probiotics in restoring microbiota dysbiosis, modulating the gut microbiome may be an effective strategy for neuropsychiatric disorders therapy. We found that the EcN-GadABC@Fe-NE/AMF treatment significantly changed the structure and composition of the gut microbiome. Gavage of EcN-GadABC@Fe-NE increased the abundance of gut probiotics, such as *Ligilactobacillus* and *Lactobacillus*, and reduced the abundance of *Alistipes* and *Desulfovibrio*. In support of our results, supplementation with *Lactobacillus* as well as its metabolites, the short-chain fatty acids (SCFAs), has been shown to exert robust anxiolytic effects [55–58]. In addition to promoting the dominance of *Lactobacillus*, EcN-GadABC@Fe-NE also reduces the abundance of *Alistipes*, a genus previously associated with anxiety- and depressive-like behaviors through reducing the availability of serotonin in mice [59–64]. Interestingly, we found that antibiotic pretreatment attenuated only certain behavioral improvements induced by the engineered probiotic, suggesting the involvement of multiple mechanisms. Taken together, our results indicated a dual mechanism of the EcN-GadABC@Fe-NE/AMF, on suppressing the activity of neural networks involved in anxiety-like behaviors and acting as a probiotic, providing beneficial effects on maintaining a balanced gut microbiota.

In summary, we have developed a nanomaterial-modified engineered probiotic EcN-GadABC@Fe-NE capable of modulating the gut-brain axis and alleviating anxiety-like behaviors under the stimulation of AMF. The probiotic acted as a dual-functional living biotherapeutic, simultaneously modulating anxiety neural networks and maintaining gut microbiota homeostasis. Our approach described here provides a novel aspect in development of therapeutic strategies for anxiety as well as other disorders of gut-brain interactions.

Supplementary Information

The online version contains supplementary material available at https://doi.org/10.1186/s12951-025-03551-3.

Supplementary Material 1

Author contributions

X.W.: Formal analysis, Data curation, Methodology, Writing – original draft. YHan.Z.,Yhao Z., Y.C., G.X.,K.C.,C.F. and Z.H.: Visualization, Validation. X.L.: Supervision, Funding acquisition. D.Z.: Conceptualization, Resources, Project administration, Writing – review & editing. All authors reviewed the manuscript.

Funding

This work was supported by the Special Foundation for Taishan Scholars (tsqn202211283), the Natural Science Foundation of Shandong Province (ZR2023QH322, ZR2019ZD33), the Research Project of Jinan Microecological Biomedicine Shandong Laboratory (JNL-202203Q), the National Natural Science Foundation of China (82071512), and Shandong Provincial Laboratory Project (SYS202202).

Data availability

No datasets were generated or analysed during the current study.

Declarations

Ethics approval and consent to participate

This study was executed under ethical approvals from the Tab of Animal Experimental Ethical Inspection of Jinan Microecological Biomedicine Shandong Laboratory.

Consent for publication

Not applicable.

Competing interests

The authors declare no competing interests.

Received: 11 December 2024 / Accepted: 16 June 2025
Published online: 01 July 2025

References

1. Disease GBD, Injury I, Prevalence C. Global, regional, and National incidence, prevalence, and years lived with disability for 328 diseases and injuries for 195 countries, 1990–2016: a systematic analysis for the global burden of disease study 2016. Lancet (London England). 2017;390(10100):1211–59.
2. Penninx BWJH, Pine DS, Holmes EA, Reif A. Anxiety disorders. Lancet. 2021;397(10277):914–27.
3. Domschke K, Stevens S, Pfleiderer B, Gerlach AL. Interoceptive sensitivity in anxiety and anxiety disorders: an overview and integration of Neurobiological findings. Clin Psychol Rev. 2010;30(1):1–11.
4. Paulus MP, Stein MB. Interoception in anxiety and depression. Brain Struct Funct. 2010;214(5–6):451–63.
5. Bonaz B, Lane RD, Oshinsky ML, Kenny PJ, Sinha R, Mayer EA, et al. Diseases, disorders, and comorbidities of interoception. Trends Neurosci. 2021;44(1):39–51.
6. Bonaz B, Bazin T, Pellissier S. The vagus nerve at the interface of the microbiota-gut-brain axis. Front Neurosci. 2018;12:49.
7. Liu L, Zhu G. Gut-Brain Axis and mood disorder. Front Psychiatry. 2018;9:223.
8. Aburto MR, Cryan JF. Gastrointestinal and brain barriers: unlocking gates of communication across the microbiota-gut-brain axis. Nat Rev Gastroenterol Hepatol. 2024;21(4):222–47.
9. Tysoe O. Mapping neuron functions in the gut-brain axis. Nat Rev Endocrinol. 2021;17(8):448.
10. Bai L, Mesgarzadeh S, Ramesh KS, Huey EL, Liu Y, Gray LA, et al. Genetic identification of vagal sensory neurons that control feeding. Cell. 2019;179(5):1129–e114323.
11. Schwartz GJ. The-pole of Gastrointestinal vagal afferents in the control of food intake: current prospects. Nutrition. 2000;16(10):866–73.
12. Han W, Tellez LA, Perkins MH, Perez IO, Qu T, Ferreira J, et al. A neural circuit for gut-induced reward. Cell. 2018;175(3):665–e67823.
13. Krieger JP, Asker M, van der Velden P, Boerchers S, Richard JE, Maric I, et al. Neural pathway for gut feelings: vagal interoceptive feedback from the Gastrointestinal tract is a critical modulator of anxiety-like behavior. Biol Psychiatry. 2022;92(9):709–21.
14. Suarez AN, Hsu TM, Liu CM, Noble EE, Cortella AM, Nakamoto EM, et al. Gut vagal sensory signaling regulates hippocampus function through multi-order pathways. Nat Commun. 2018;9(1):2181.
15. Benarroch EE. The central autonomic network - functional-organization, dysfunction, and perspective. Mayo Clin Proc. 1993;68(10):988–1001.

16. Lyte M, Li W, Opitz N, Gaykema RPA, Goehler LE. Induction of anxiety-like behavior in mice during the initial stages of infection with the agent of murine colonic hyperplasia *Citrobacter rodentium*. Physiol Behav. 2006;89(3):350–7.
17. Goehler LE, Gaykema RPA, Opitz N, Reddaway R, Badr N, Lyte M. Activation in vagal afferents and central autonomic pathways: early responses to intestinal infection with *Campylobacter jejuni*. Brain Behav Immun. 2005;19(4):334–44.
18. Hosoi T, Okuma Y, Nomura Y. Electrical stimulation of afferent vagus nerve induces IL-1beta expression in the brain and activates HPA axis. Am J Physiol Regul Integr Comp Physiol. 2000;279(1):R141–7.
19. Klarer M, Arnold M, Guenther L, Winter C, Langhans W, Meyer U. Gut vagal afferents differentially modulate innate anxiety and learned fear. J Neurosci. 2014;34(21):7067–76.
20. Egerod KL, Petersen N, Timshel PN, Rekling JC, Wang Y, Liu Q, et al. Profiling of G protein-coupled receptors in vagal afferents reveals novel gut-to-brain sensing mechanisms. Mol Metab. 2018;12:62–75.
21. Ho CL, Tan HQ, Chua KJ, Kang A, Lim KH, Ling KL, et al. Engineered commensal microbes for diet-mediated colorectal-cancer chemoprevention. Nat Biomed Eng. 2018;2(1):27–37.
22. Motta J-P, Bermudez-Humaran LG, Deraison C, Martin L, Rolland C, Rousset P et al. Food-grade bacteria expressing Elafin protect against inflammation and restore colon homeostasis. Sci Transl Med. 2012;4(158).
23. Isabella VM, Ha BN, Castillo MJ, Lubkowicz DJ, Rowe SE, Millet YA, et al. Development of a synthetic live bacterial therapeutic for the human metabolic disease phenylketonuria. Nat Biotechnol. 2018;36(9):857–64.
24. Harimoto T, Hahn J, Chen YY, Im J, Zhang J, Hou N, et al. A programmable encapsulation system improves delivery of therapeutic bacteria in mice. Nat Biotechnol. 2022;40(8):1259–69.
25. Guo P, Wang W, Xiang Q, Pan C, Qiu Y, Li T, et al. Engineered probiotic ameliorates ulcerative colitis by restoring gut microbiota and redox homeostasis. Cell Host Microbe. 2024;32(9):1502–e15189.
26. Liu WZ, Zhang WH, Zheng ZH, Zou JX, Liu XX, Huang SH, et al. Identification of a prefrontal cortex-to-amygdala pathway for chronic stress-induced anxiety. Nat Commun. 2020;11(1):2221.
27. Ducarmon QR, Zwittink RD, Hornung BVH, van Schaik W, Young VB, Kuijper EJ. Gut microbiota and colonization resistance against bacterial enteric infection. Microbiol Mol Biol Rev. 2019;83(3).
28. Centurion F, Basit AW, Liu J, Gaisford S, Rahim MA, Kalantar-Zadeh K. Nanoencapsulation for probiotic delivery. ACS Nano. 2021;15(12):18653–60.
29. Hong S, Kim J, Na YS, Park J, Kim S, Singha K, et al. Poly(norepinephrine): ultrasmooth material-independent surface chemistry and nanodepot for nitric oxide. Angew Chem Int Ed Engl. 2013;52(35):9187–91.
30. Abdou AM, Higashiguchi S, Horie K, Kim M, Hatta H, Yokogoshi H. Relaxation and immunity enhancement effects of γ-Aminobutyric acid (GABA) administration in humans. BioFactors. 2006;26(3):201–8.
31. Cryan JF, Dinan TG. Mind-altering microorganisms: the impact of the gut microbiota on brain and behaviour. Nat Rev Neurosci. 2012;13(10):701–12.
32. Landry BP, Tabor JJ. Engineering diagnostic and therapeutic gut bacteria. Microbiol Spectr. 2017;5(5):10.
33. Riglar DT, Silver PA. Engineering bacteria for diagnostic and therapeutic applications. Nat Rev Microbiol. 2018;16(4):214–25.
34. Pan H, Sun T, Cui M, Ma N, Yang C, Liu J, et al. Light-Sensitive *Lactococcus lactis* for microbe-gut-brain axis regulating via upconversion optogenetic micro-nano system. ACS Nano. 2022;16(4):6049–63.
35. Riglar DT, Giessen TW, Baym M, Kerns SJ, Niederhuber MJ, Bronson RT, et al. Engineered bacteria can function in the mammalian gut long-term as live diagnostics of inflammation. Nat Biotechnol. 2017;35(7):653–8.
36. Taketani M, Zhang J, Zhang S, Triassi AJ, Huang YJ, Griffith LG, et al. Genetic circuit design automation for the gut resident species *Bacteroides thetaiotaomicron*. Nat Biotechnol. 2020;38(8):962–9.
37. Piraner DI, Abedi MH, Moser BA, Lee-Gosselin A, Shapiro MG. Tunable thermal bioswitches for in vivo control of microbial therapeutics. Nat Chem Biol. 2017;13(1):75–80.
38. Moros M, Idiago-López J, Asín L, Moreno-Antolín E, Beola L, Grazú V, et al. Triggering antitumoural drug release and gene expression by magnetic hyperthermia. Adv Drug Deliv Rev. 2019;138:326–43.
39. Wu F, Liu J. Decorated bacteria and the application in drug delivery. Adv Drug Deliv Rev. 2022;188:114443.
40. Cao Z, Wang X, Pang Y, Cheng S, Liu J. Biointerfacial self-assembly generates lipid membrane coated bacteria for enhanced oral delivery and treatment. Nat Commun. 2019;10(1):5783.
41. Anselmo AC, McHugh KJ, Webster J, Langer R, Jaklenec A. Layer-by-layer encapsulation of probiotics for delivery to the Microbiome. Adv Mater. 2016;28(43):9486–90.
42. Goehler LE, Gaykema RP, Opitz N, Reddaway R, Badr N, Lyte M. Activation in vagal afferents and central autonomic pathways: early responses to intestinal infection with *Campylobacter jejuni*. Brain Behav Immun. 2005;19(4):334–44.
43. Krieger JP, Asker M, van der Velden P, Börchers S, Richard JE, Maric I, et al. Neural pathway for gut feelings: vagal interoceptive feedback from the Gastrointestinal tract is a critical modulator of anxiety-like behavior. Biol Psychiatry. 2022;92(9):709–21.
44. Herman JP, Figueiredo H, Mueller NK, Ulrich-Lai Y, Ostrander MM, Choi DC, et al. Central mechanisms of stress integration: hierarchical circuitry controlling hypothalamo-pituitary-adrenocortical responsiveness. Front Neuroendocrinol. 2003;24(3):151–80.
45. Bains JS, Wamsteeker Cusulin JI, Inoue W. Stress-related synaptic plasticity in the hypothalamus. Nat Rev Neurosci. 2015;16(7):377–88.
46. Holt MK. The Ins and outs of the caudal nucleus of the solitary tract: an overview of cellular populations and anatomical connections. J Neuroendocrinol. 2022;34(6):e13132.
47. McCall JG, Al-Hasani R, Siuda ER, Hong DY, Norris AJ, Ford CP, Bruchas MR. CRH engagement of the locus coeruleus noradrenergic system mediates Stress-Induced anxiety. Neuron. 2015;87(3):605–20.
48. McCall JG, Siuda ER, Bhatti DL, Lawson LA, McElligott ZA, Stuber GD, et al. Locus coeruleus to basolateral amygdala noradrenergic projections promote anxiety-like behavior. Elife. 2017;6:e18247.
49. Zerbi V, Floriou-Servou A, Markicevic M, Vermeiren Y, Sturman O, Privitera M, et al. Rapid reconfiguration of the functional connectome after chemogenetic locus coeruleus activation. Neuron. 2019;103(4):702–e185.
50. Sciolino NR, Plummer NW, Chen YW, Alexander GM, Robertson SD, Dudek SM, et al. Recombinase-dependent mouse lines for chemogenetic activation of genetically defined cell types. Cell Rep. 2016;15(11):2563–73.
51. McCall JG, Al-Hasani R, Siuda ER, Hong DY, Norris AJ, Ford CP, et al. CRH engagement of the locus coeruleus noradrenergic system mediates stress-induced anxiety. Neuron. 2015;87(3):605–20.
52. Lee B, Shim I, Lee H, Hahm DH. Effect of ginsenoside re on depression- and anxiety-like behaviors and cognition memory deficit induced by repeated immobilization in rats. J Microbiol Biotechnol. 2012;22(5):708–20.
53. Lee B, Yun HY, Shim I, Lee H, Hahm DH. *Bupleurum falcatum* prevents depression and anxiety-like behaviors in rats exposed to repeated restraint stress. J Microbiol Biotechnol. 2012;22(3):422–30.
54. Navarro-Tapia E, Almeida-Toledano L, Sebastiani G, Serra-Delgado M, Garcia-Algar O, Andreu-Fernandez V. Effects of microbiota imbalance in anxiety and eating disorders: probiotics as novel therapeutic approaches. Int J Mol Sci. 2021;22(5):2351.
55. Kozin SV, Kravtsov AA, Kravchenko SV, Ivashchenko LI. Antioxidant and anxiolytic effect of *Bifidobacterium adolescentis* and *Lactobacillus acidophilus* under conditions of Normobaric hypoxia with hypercapnia. Vopr Pitan. 2021;90(2):63–72.
56. Niu Y, Liang S, Wang T, Hu X, Li W, Wu X, Jin F. Pre-Gestational intake of *Lactobacillus helveticus* NS8 has anxiolytic effects in adolescent Sprague Dawley offspring. Brain Behav. 2020;10(9):e01714.
57. Olorocisimo JP, Diaz LA, Co DE, Carag HM, Ibana JA, Velarde MC. *Lactobacillus delbrueckii* reduces anxiety-like behavior in zebrafish through a gut microbiome-brain crosstalk. Neuropharmacology. 2023;225:109401.
58. Zheng KY, Gao B, Wang HJ, He JG, Chen HS, Hu ZL, et al. Melatonin ameliorates depressive-like behaviors in ovariectomized mice by improving Tryptophan metabolism via Inhibition of gut microbe *Alistipes Inops*. Adv Sci (Weinh). 2024;11(34):e2309473.
59. Song X, Wang W, Ding S, Liu X, Wang Y, Ma H. Puerarin ameliorates depression-like behaviors of with chronic unpredictable mild stress mice by remodeling their gut microbiota. J Affect Disord. 2021;290:353–63.
60. Simpson CA, Diaz-Arteche C, Eliby D, Schwartz OS, Simmons JG, Cowan CSM. The gut microbiota in anxiety and depression - A systematic review. Clin Psychol Rev. 2021;83:101943.
61. van de Wouw M, Boehme M, Lyte JM, Wiley N, Strain C, O'Sullivan O, Clarke G, Stanton C, Dinan TG, Cryan JF. Short-chain fatty acids: microbial metabolites that alleviate stress-induced brain-gut axis alterations. J Physiol. 2018;596(20):4923–44.
62. Chen H, Zhang L, Li Y, Meng X, Chi Y, Liu M. Gut microbiota and its metabolites: the emerging Bridge between coronary artery disease and anxiety and depression? Aging Dis. 2024;16(3):1265–84.

63. Jiang H, Ling Z, Zhang Y, Mao H, Ma Z, Yin Y, et al. Altered fecal microbiota composition in patients with major depressive disorder. Brain Behav Immun. 2015;48:186–94.
64. Navarro-Tapia E, Almeida-Toledano L, Sebastiani G, Serra-Delgado M, García-Algar Ó, Andreu-Fernández V. Effects of microbiota imbalance in anxiety and eating disorders: probiotics as novel therapeutic approaches. Int J Mol Sci. 2021;22(5):2351.

Publisher's note